Journal of the Korean Ceramic Society
Vol. 43, No. 9, pp. 519~526, 2006.

Optimization of Barium Titanate Slip for Tape Casting Using Design of Experiments

Sung-Wook Kwon, Nono Darsono, and Dang-Hyok Yoon†

School of Materials Science and Engineering, Yeungnam University, Gyeongsan 712-749, Korea
(Received July 9, 2006; Accepted August 22, 2006)

ABSTRACT

A full-factorial design of experiments with three input factors and two levels for each factor including center points was utilized for the preparation and characterization of twelve types of $BaTiO_3$ slips for tape casting. Ceramic powders with different particle sizes, different milling methods such as high energy milling and conventional ball milling, and two types of dispersant with different polymeric species were chosen as input factors in order to investigate their effects on slip and on green tape properties. Tape casting, a small rectangular-shaped K-square preparation, characterization and quantitative data analysis using statistical software were followed. Ceramic powder was the most significant among three input factors for the output responses of slip viscosity and green tape density, showing more favorable results with large particles than with very fine ones. In addition, high energy milling for only 30 min was more efficient than 24 h of conventional ball milling in terms of powder dispersion and milling. The optimum condition based on the experimental results was a slip exposed to high energy milling with large ceramic particles along with a methylethyl acetate dispersant.

Key words*: *Tape casting, Barium titanate, Milling, Green density, Viscosity

1. Introduction

Tape casting has been widely used for the fabrication of thin ceramic sheets since Howatt et al. described the process in 1947.[1] Basically, acquiring a high-quality tape consists of the preparation of a stable slip of ceramic powder in binder solution. Desirable tape properties include a smooth and densely packed green surface morphology, adequate strength for further processing, no defects such as pinholes or fisheyes, and a uniform thickness with well-dispersed ceramic particles. The main ingredients of the slip are the ceramic powder, binder, liquid medium, dispersant and plasticizer, with compatibility among polymeric additives very important.[2,3] In addition, the average molecular weight and the amount of polymeric additives are also important. The characteristics of a ceramic powder and a liquid medium must also be seriously considered.[4] Depending on the impurity level, average size, shape and size distribution of the ceramic powder, the final tape properties can vary. The liquid medium should dissolve all of the polymeric additives, such as the binder resin, with low surface tension for a complete wetting and fast drying of a cast tape.[5]

Fine ceramic powder tends to agglomerate due to their high specific surface area, which should be dispersed in order to obtain a high quality slip. By means of mechanical energy such as impact and shear forces, the agglomerates are usually broken into smaller particles. Conventional ball mills and attrition mills adopting a discontinuous operating system have been used extensively for this purpose. On the other hand, modern high energy mills use a continuous operating system equipped with a high speed rotor turning at up to several thousands of rotations per minute (rpm), disc agitators and a cooling system. Their high energy input along with the use of small grinding media with diameters of 0.05-0.5 mm allow for the achievement of very small particle sizes in the nanometer range and of a highly dispersed ceramic slip in a very short processing time.[6] As high energy mill using very fine media has been recently introduced, however, there are few reports thus far regarding its efficiency in terms of slip preparation compared to conventional ball milling. The schematic of a high energy mill[7] is shown in Fig. 1.

As shown above, investigations regarding on adequate slip formulation involve many experimental input factors. Design of experiments (DOE) is a very powerful tool for establishing relationships among many input factors and output responses for such a complex system. DOE is an experimental method using a structured plan in which the input factors vary in a planned manner in order to efficiently optimize output responses of interest with minimal variability. A subsequent interpretation of the data based on an analysis of variance (ANOVA) will identify the input factors that most influence the results as well as those that do not; it will also identify the presence of interactions

†Corresponding author : Dang-Hyok Yoon
E-mail : dhyoon@ynu.ac.kr
Tel : +82-53-810-2561 Fax : +82-53-810-4628

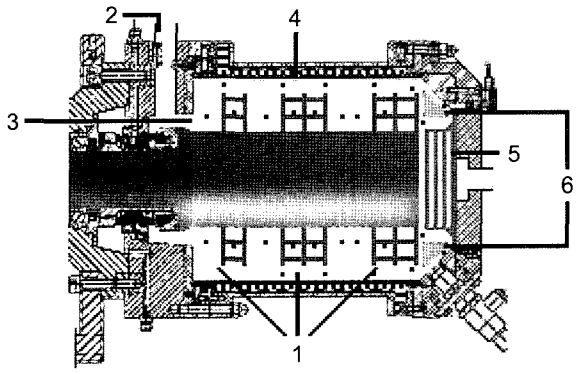

Fig. 1. Schematic of the grinding chamber of the high energy mill.[7] 1: Rotor with discs, 2: inlet, 3: grinding media, 4: cooling jacket, 5 and 6: separation system.

among the input factors.[8] The next step is optimization, which leads to the best possible output response by choosing adequate levels of input factors. Levels signify different values that input factors take in an experiment. Mathematics and computers are usually needed for an analysis of the data to keep track of the factors and their combinations in DOE.

Depending on what is already known about the problem, different classes of designs are used for laying out the set of experiments. Fractional factorial designs use only a well-balanced subset of the possible combinations of levels of factors. This is particularly recommended when most of the quantities of interest can still be estimated using smaller types of experiment. Full factorial designs use all combinations of the chosen levels of the chosen factors. These are very practical and are easy to understand but require numerous experimental runs when the numbers of input factors are large. Response Surface Methods (RSM) are used later in an investigation for the final optimization, and when one wishes to develop a model relating the dominating factors to the response variables.[9] As we move down this list, the experiments generate more powerful data at the expense of larger experimental designs, more samples, or increased complexity. A great deal of care must be taken in selecting the design, input factors and factor levels in order to be able to answer as many of a researcher's questions as possible.

Based on this background, therefore, a full factorial DOE is performed in this work in order to determine an optimum $BaTiO_3$ slip condition for tape casting using three experimental input factors with two levels for each factor: $BaTiO_3$ powders with different average particle sizes, different milling methods such as a conventional ball milling and a high energy milling, and two different types of dispersant. Twelve runs of experiments were performed in this experiment by adding center points with ceramic powder, although eight runs were needed for a full factorial design without center points. One of the concerns in the use of two-level factorial design is the assumption of linearity in the output response between low and high levels of input factors. Therefore, a center point having the exact mid-value between two levels is typically added in order to establish the existence of curvature in the output response. Statistical analysis software, MINITAB, is used for the generation of DOE table and for the analysis of the results. The effect of each input factor on output responses of the slip viscosity, green tape density and green morphology are described in this paper through ANOVA results, main effect plots, and electron microscope images.

2. Experimental Procedure

$BaTiO_3$ powders, milling methods and dispersants were chosen as controlled factors. Two types of $BaTiO_3$ powders with different average particle sizes were used: the first was the hydrothermally produced BT-01 (Sakai Chemicals, Japan) with an average particle size of 99 nm, a specific surface area of 12.36 m^2/g and a Ba/Ti ratio of 0.994. The second was SBT-045 (Samsung Fine Chemicals, Korea) produced via an oxalate method with the corresponding values of 407 nm, 2.31 m^2/g and 0.999, respectively. Both powders have spherical morphology with a large difference in the particle size. Their SEM images are shown in Fig. 2. In order to characterize the packing properties, the tap density was measured after five minute of tapping using plastic cylinders for 100 g of BT-01 and SBT-045, with a 50/50 wt%

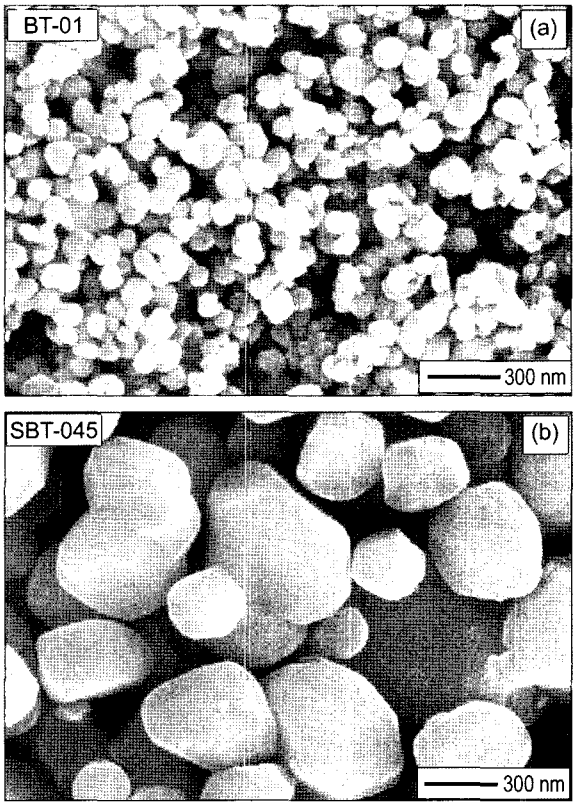

Fig. 2. SEM micrographs of commercial $BaTiO_3$ powder: (a) BT-01 produced by hydrothermal method, and (b) SBT-045 by oxalate method.

mixture of both powders. Sedimentation densities for 10 g of both powders and a mixture were also measured after maintaining the suspensions for three weeks in glass cylinders of different liquid media of ethanol, toluene and a 60/40 wt% of toluene/ethanol mixture added with different dispersants. The two different milling methods used were conventional ball milling for 24 h with 2 mm Yittria-Stablilized Zirconia (YSZ) media at 95 rpm using 500 cc Nalgene bottle, and high energy milling (MiniCer, Netzsch, Germany) at 3,000 rpm for 30 min with 0.40 mm YSZ beads. Phosphate esters-based Rhodafac RE-610 (Rhodia, Korea) and methylethyl acetate-based Disperbyk-103 (BYK-Chemie, USA) were used as dispersants. In order to verify the mixing effects of two types of ceramic powders, ceramic powder mixed with identical amounts of BT-01 and SBT-045 was chosen as the center point. Table 1 presents twelve runs of the full factorial design table generated by MINITAB for three factors and two levels with center points.

Polyvinyl butyral (PVB) resin with an average molecular weight of 55,000 g/mole (B-98, Solutia, USA) was used as a binder phase. PVB is commercially prepared by an acid-catalyzed butyr-aldehyde condensation reaction with polyvinyl alcohol (PVA). The resulting product typically contains a small amount of PVA and polyvinyl acetate due to the incomplete condensation reaction.[10,11] All of the materials used in this experiment, including the molecular structure of the binder system, are listed in Table 2.

Twelve different types of ceramic slips were prepared via the multi-step process described below. To initially prepare a binder solution, 250 g of PVB resin was dissolved in 2,500 g of 60/40 (wt%) toluene/ethanol mixture. Following this, 40 wt% of dioctyl phthalate (DOP) with respect to the weight of PVB resin was added as a plasticizer which provides a plastic flow to the slip. This binder solution was stirred overnight at room temperature after sealing the bottle in order to minimize the evaporation of solvents. Next, 0.5 wt% of the dispersant corresponding to the Table 1 was added to 12 bottles of 228 g each of binder solution. 200 g of BT-01 or SBT-045 was added to these binder solutions, as outlined in Table 1, in order to create a binder resin ratio of 10 wt% with respect to the ceramic powder. Ball milling or high energy milling was performed at each condition

Table 1. Twelve Runs of the DOE Table Generated by Minitab

Run	Center point	Experimental factors and levels		
		$BaTiO_3$ powder	Milling	Dispersant
1	1	BT-01	Ball mill	RE 610
2	1	SBT-045	Ball mill	RE 610
3	1	BT-01	High E mill	RE 610
4	1	SBT-045	High E mill	RE 610
5	1	BT-01	Ball mill	BYK 103
6	1	SBT-045	Ball mill	BYK 103
7	1	BT-01	High E mill	BYK 103
8	1	SBT-045	High E mill	BYK 103
9	0	BT-01+SBT-045	Ball mill	RE 610
10	0	BT-01+SBT-045	High E mill	RE 610
11	0	BT-01+SBT-045	Ball mill	BYK 103
12	0	BT-01+SBT-045	High E mill	BYK 103

Table 2. Materials Information Used in This Experiment

Materials	Description
$BaTiO_3$ powder	
BT-01	D_{mean}=99 nm, BET=12.36 m^2/g, Ba/Ti=0.994, Hydrothermal
SBT-045	D_{mean}=407 nm, BET=2.31 m^2/g, Ba/Ti=0.999, Oxalate
Binder system	
Binder resin	Polyvinyl butyral (PVB), T_g=75°C, MW=55,000 g/mole
Dispersant	RE-610: Phosphate esters (Nonylphenol ethoxylate-based)
	BYK-103: Copolymer with methylethyl acetate
Plasticizer	Dioctyl phthalate
Solvent	Toluene/ethanol=6/4 in weight-base

Molecular structure of PVB binder system

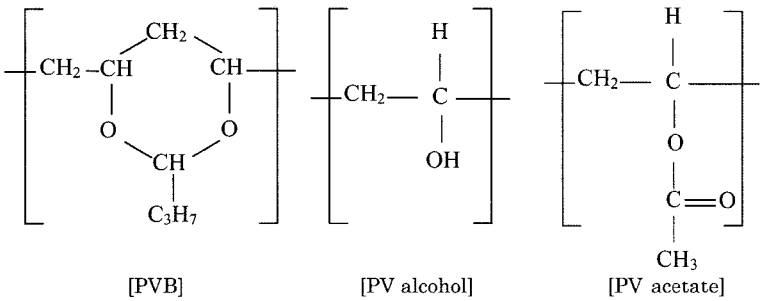

[PVB] [PV alcohol] [PV acetate]

explained above for the twelve slips.

The rheological behavior of the prepared slips was investigated using a viscometer (DV-II, Brookfield, USA) using a LV-3 spindle at 25°C in the rotation speed of 1-60 rpm. Tape casting followed on a moving polyester film using a table top tape caster with a casting rate of 60 cm/min. The cast tapes were dried at an air flow temperature of 80°C, and the resultant green tape thickness was measured as 15-25 μm. The green microstructure of the tapes was observed using a Scanning Electron Microscope (SEM; Hitachi S-4100) after platinum coating. The green density of the tapes was measured via a geometrical method after the preparation of eight K-squares for each condition. Each K-square was a small rectangular-shaped specimen (1.2×1.2 cm^2) produced by the stacking the green tapes into 1 mm thickness, pressing under 300 kPa at 90°C, and cutting the pressed green plate. The thickness and length were measured using a micrometer accurate to 0.001 mm and the weight was measured using a scale accurate to 0.1 mg. A schematic of the experimental procedure is given in Fig. 3.

3. Results and Discussion

Tap density measurement is one of the simplest methods for determining the packing properties of powder. Even powders with similar particle sizes usually show different tap densities due to their morphologies and degree of surface roughness. The tap densities of BT-01, SBT-045 and the mixture of both powders are shown in Fig. 4. BT-01 shows the lowest tap density of 1.25 g/cm^3, which corresponds to 20.66% of the theoretical $BaTiO_3$ density (6.05 g/cm^3). The highest density of 1.56 g/cm^3 is shown with SBT-045, and the mixed powder shows an intermediate value of

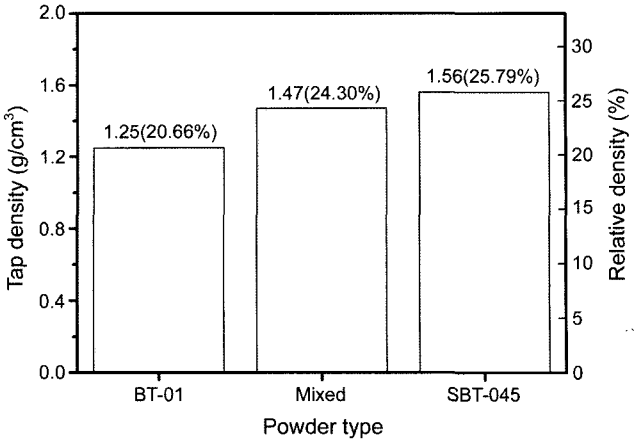

Fig. 4. Tap densities of BT-01, SBT-045 and the mixture of both powders.

1.47 g/cm^3. However, these values are much lower than the packing density of simple cubic (52%) or non-ordered arrangements (60%) measured with uniform spheres larger than 1 mm.[12] A higher tap density for the mixed powder was expected, as the small BT-01 could be distributed in the interstices of large SBT-045 particles based on Furnas model.[13] However, bridging and agglomerating of fine particles with rough surfaces appear to prevent the particles from a rearrangement for high packing density.

The box-plot in Fig. 5 shows the sedimentation density of the suspensions as a function of the ceramic powders, solvents and dispersants. A line is drawn across the box at the median, and the dot inside the box indicates the mean. By default, the bottom of the box is at the first quartile, and the top is at the third quartile value. The whiskers are the

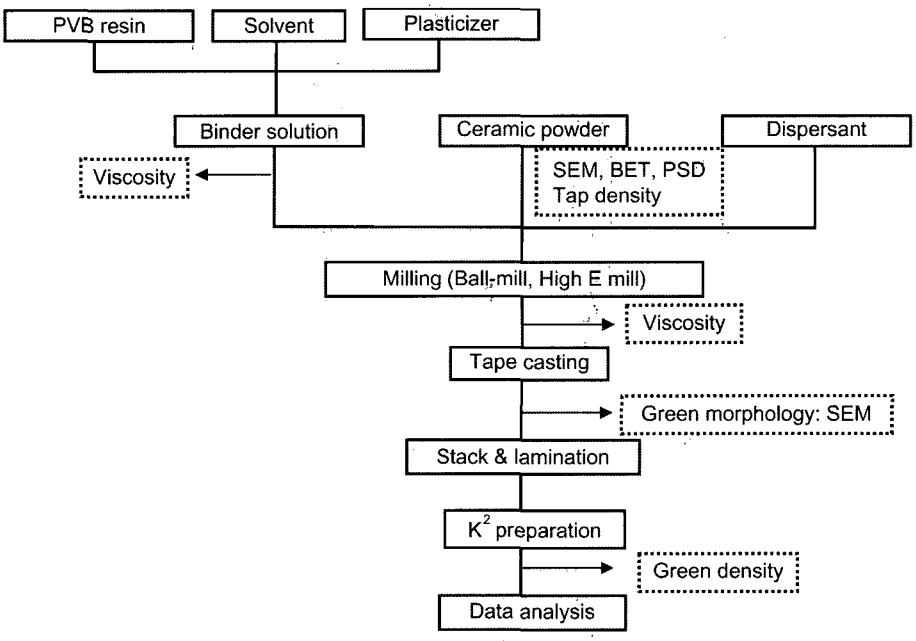

Fig. 3. Schematic of the experimental procedure.

lines that extend from the top and bottom of the box to the lowest and highest observations inside the inner and outer fences. The values of the sedimentation densities are in the range of 0.86 to 2.68 g/cm^3, which are 14-44% of the theoretical $BaTiO_3$ density. The average sedimentation density vs. ceramic powder shows identical behavior to that of the tap density with dried powder: SBT-045>mixed powder>BT-01, which illustrates the importance of the powder characteristics in sedimentation. Although the sedimentation density in ethanol shows the highest value, mixed solvents are used in this experiment as they show a higher solubility to the binder resin and a faster drying rate compared to ethanol only.[5] By adding 0.5 wt% of dispersant in the suspension, the sedimentation density is increased as shown in the figure. It is known that steric repulsion is more effective than electrostatic repulsion in solvent-based systems due to the lower ionic strength and dielectric constant of solvent compared to those of water.[5] Therefore, the increase in sedimentation density of the powder with the dispersant results from the polymeric stabilization which comes from the repulsion forces caused by the dispersant covering the powder surface. As the variance in sedimentation density is large due to the interactions among experimental factors and other noises, as shown in Fig. 5, the clarification above explains the overall trend.

The binder solution without ceramic powder shows Newtonian rheological behavior with a viscosity of 55 mPa·s regardless of the shear rate. On the other hand, all of the slips containing ceramic powder represent pseudo-plastic behavior showing a decrease in the viscosity with an increase in the shear rate, as shown in Fig. 6. Slips with fine BT-01 generally show high viscosity, while those with coarse SBT-045 or with high energy milling show low viscosity, implying better dispersion. Efforts were made to keep the systems as similar as possible to one another in terms of their final slip composition for the comparison, as shown in Table 3. In order to verify the effect of each input factor, a main effects plot for slip viscosity is shown in Fig. 7.

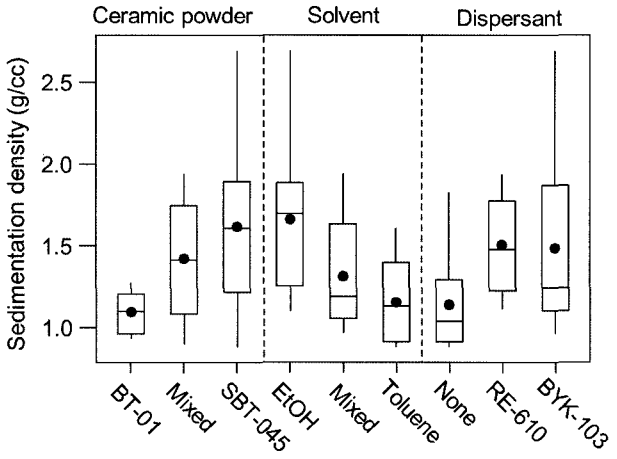

Fig. 5. Sedimentation densities of suspensions as a function of the ceramic powders, solvents and dispersants.

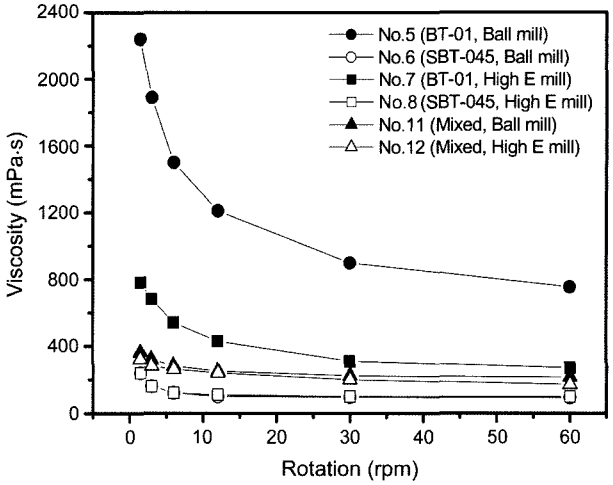

Fig. 6. Rheological behavior of slips with the BYK-103 dispersant on different ceramic powders and milling methods.

Table 3. Slip Composition Including Ceramic Powder, Polymer, and Liquid Medium

Type	Content (wt%)
Ceramic powder	46.46-46.62
Polymer	7.99-8.08
Liquid medium	45.39-45.47

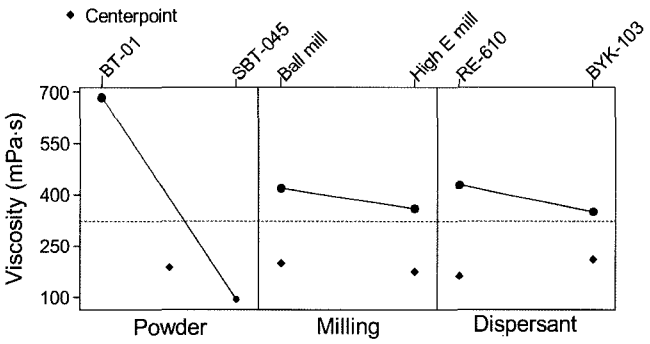

Fig. 7. Main effects plot of the slip viscosity as a function of the experimental input factors.

A dashed reference line is drawn at the grand mean of the viscosity data, and circle symbols in the graph are the means of the slip viscosity at two levels of each input factor. The diamond symbols represent center points which correspond to the viscosities of powder mixture under given conditions. If the diamond symbol lies on or near the lines connecting the effect averages, it would be possible to conclude that there is little curvature in the experiment. If the symbol lies far from the lines, the conclusion is that there is some measure of curvature in the system. Ceramic powder, showing the steepest slope between the two levels, is the most significant factor among the three input factors, showing a much lower viscosity with the slips containing SBT-045 than with those containing BT-01. The center point, i.e. the viscosity of the mixture, is located between the viscosi-

ties of BT-01 and SBT-045, although it does not show an exact linear relationship with the relative amount of each powder. Slips exposed to high energy milling for only 30 min show a slightly lower viscosity than those with ball milling for 24 h, which illustrates the high efficiency of this method in terms of dispersion. Although the effect of the dispersants is relatively small, slips with BYK-103 shows a lower viscosity compared to those with RE-610. Therefore, it can be concluded that the optimum slip condition for low viscosity is a combination of coarse SBT-045 powder subjected to the high energy milling with a BYK-103 dispersant. The low slip viscosity is preferred as it is possible to increase the solid loading of a slip in order to obtain a high green tape density.[4]

A main effects plot of the green density as a function of the experimental input factors is shown in Fig. 8. The green density values are within the range of 3.07-3.70 g/cm^3, or 51-61% of the theoretical density of $BaTiO_3$. Ceramic powder is the most significant factor on the green tape density: tapes with SBT-045 show a higher density than those with fine BT-01, indicating a better dispersion and packing property with SBT-045. Regarding the effect of milling, tapes exposed to high energy milling show a higher density than those with ball milling. The effect of a dispersant on the green density is insignificant for slips with each powder, while BYK-103 is shown to be very efficient for a mixed powder system. Tapes with high green density are generally preferred, especially for applications demanding very thin tapes such as those in the Multi-Layer Ceramic Capacitor (MLCC) industry.[14]

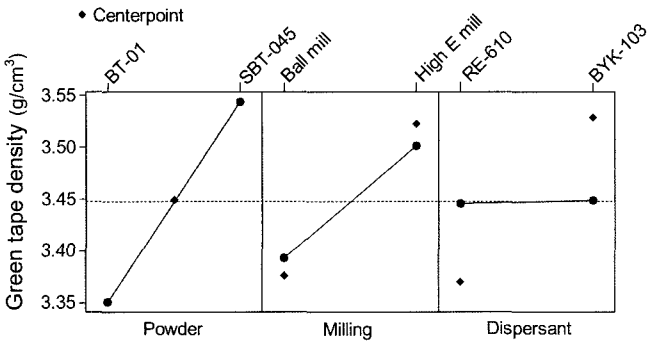

Fig. 8. Main effects plot of the green tape density as a function of the experimental input factors.

An MLCC having the highest volumetric efficiency is currently as thin as 1 μm and is comprised of several hundreds of dielectric layers, for example, with this expected to become thinner in the future in order to replace Ta and Al electrolytic capacitors.[15-17] As the general belief is that each sintered layer of MLCC requires at least five grains to ensure reliability,[14,18] $BaTiO_3$ powder with an average particle size of less than 200 nm is desirable. If one of the dielectric layers contains pores that originate from poor powder dispersion, failure of the final MLCC occurs. Considering the above results, however, it is estimated that dispersion is becoming difficult with fine particles, explaining why all researchers are now trying to obtain better dispersion of a slip and higher green density of a tape in the MLCC industry.

The surface morphologies of the green tapes prepared with BYK-103 using different ceramic powders and milling methods are shown in Fig. 9. By comparing Fig. 9(a) and (c), it is clear that the green tape with high energy milled BT-01 shows denser surface morphology than ball milled one with the same powder. The measured green density of the former is 3.51 g/cm^3, while that of the latter is 3.24 g/cm^3, indicating the importance of the milling process in obtaining high green density. In addition, the green density of the ball milled SBT-045 sample shown in Fig. 9(b) is 3.56 g/cm^3,

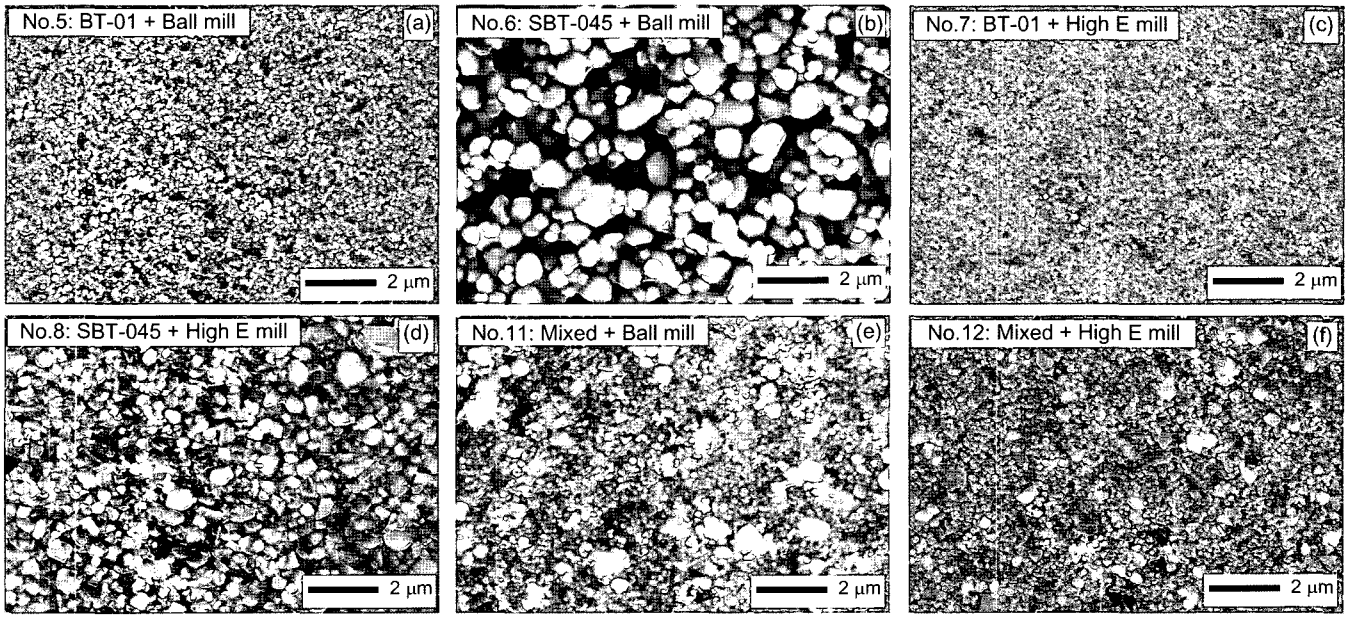

Fig. 9. Surface morphologies of green tapes with the BYK-103 dispersant for different ceramic powders and milling methods.

which is also larger than that for the ball milled BT-01 sample in Fig. 9(a). By comparing the microstructures of Fig. 9(b) and (d), both of which were prepared with SBT-045, a smoother and denser green surface is observed in high energy milled sample. Moreover, chipped particles of SBT-045 in the high energy milled tapes (Fig. 9(d) and (f)) are observed, while the particles in the ball milled tapes (Fig. 9(b) and (e)) maintain their original shape. For the tapes with the mixed powder, the high energy-milled sample (Fig. 9(f)) also shows a denser surface morphology compared to that of the ball-milled sample (Fig. 9(e)). The same trend, i.e., denser green tape morphologies with the SBT-045 powder and high energy milling over the tapes with BT-01 and ball milling, is observed for tapes with the RE-610 dispersant, although the morphologies are not shown here.

More detailed interpretations of the experimental results are possible based on an analysis of variance (ANOVA) that identifies the influence of the input factors, the presence of interactions, and the relative portion of error included. Table 4 shows the summary of the ANOVA table, showing the sum of square for each source and the resultant model equation for two output responses: slip viscosity and green tape density. According to this table, approximately 87% of the variation can be explained by main effects and two-way interactions for both output responses, and the errors included are no more than 14%. The contribution of experimental input factors, with the exception of the interactions, is 77% for the slip viscosity, while it is only 33% for the green tape density indicating that there is 53% for the two-way interactions for the green tape density. For each output response, a model equation is also shown for each source, making it easier to determine the optimum condition.[19] The optimum condition for low slip viscosity and high green density based on the results is: SBT-045 powder exposed to high energy milling along with the BYK-103 dispersant.

Table 4. ANOVA Table Showing Sum of Square for Each Source and Resultant Model Equations for Slip Viscosity and Green Tape Density

Source	Sum of square (% contribution)	
	For slip viscosity	For green tape density
Main effects	818,588 (77.0)	0.127920 (33.1)
- $BaTiO_3$ powder	807,647 (75.9)	0.074686 (19.3)
- Milling	7,125 (0.7)	0.044153 (11.4)
- Dispersant	3,816 (0.4)	0.009081 (2.4)
2-way interactions	108,009 (10.2)	0.206977 (53.4)
- $BaTiO_3$×Milling	11,221 (1.1)	0.163586 (42.2)
- $BaTiO_3$×Dispersant	25,332 (2.4)	0.021417 (5.5)
- Milling×Dispersant	71,456 (6.7)	0.021974 (5.7)
Residual error	137,002 (12.8)	0.052368 (13.5)
Total	1,063,599 (100.0)	0.387263 (100.0)

Model equation:

$$\text{Slip viscosity} = 389.7 - 295.6BaTiO_3 - 24.4\text{Milling} - 17.8\text{Dispersant} - 36.1BaTiO_3 \times \text{Milling} + 42.9BaTiO_3 \times \text{Dispersant} - 77.2\text{Milling} \times \text{Dispersant} - 201.9 \times \text{Center point}$$

$$\text{Green density} = 3.447 + 0.097BaTiO_3 + 0.060\text{Milling} + 0.028\text{Dispersant} - 0.143\ BaTiO_3 \times \text{Milling} - 0.025\ BaTiO_3 \times \text{Dispersant} - 0.043\ \text{Milling} \times \text{Dispersant}$$

4. Conclusions

The results presented above enable the following conclusions to be drawn:

1. Coarse SBT-045 showed higher tap and sedimentation densities than fine BT-01. $BaTiO_3$ powder was the most significant factor for low slip viscosity and high green tape density, consistently showing more favorable results with the large SBT-045 over the fine BT-01.
2. High energy milling at 3,000 rpm for only 30 min was more efficient than 24 h of conventional ball milling in terms of milling and dispersion efficiency, showing a lower slip viscosity and higher green tape density.
3. Approximately 87% of the variation results from the main effects and two-way interactions, while the errors included are no more than 14% for both the slip viscosity and green tape density, based on the statistical analysis. Model equations were also drawn for both the slip viscosity and green density.
4. The slip prepared with SBT-045 and the BYK-103 dispersant exposed to high energy milling is the optimum condition based on the DOE results.

REFERENCES

1. G. N. Howatt, R. G. Breckenridge, and J. M. Brownlow, "Fabrication of Thin Ceramic Sheets for Capacitors," *J. Am. Ceram. Soc.*, **30** [8] 237-42 (1947).
2. D. H. Yoon and B. I. Lee, "Processing of Barium Titanate Tapes with Different Binders for MLCC Applications-Part I: Optimization Using Design of Experiments," *J. Eur. Ceram. Soc.*, **24** 739-52 (2004).
3. D. H. Yoon and B. I. Lee, "Processing of Barium Titanate Tapes with Different Binders for MLCC Applications-Part II: Comparison of the Properties," *J. Eur. Ceram. Soc.*, **24** 753-61 (2004).
4. R. E. Mistler and E. R. Twiname, "Tape Casting Theory and Practice," pp. 10-21, The American Ceramic Society, Westerville, OH, 2000.
5. R. Moreno, "The Role of Slip Additives in Tape-Casting Technology: Part I-Solvents and Dispersants," *J. Am. Ceram. Soc. Bull.*, **71** [10] 1521-31 (1992).
6. C. Warnke, "Residence Time Distribution for Passage, Cascade, Circulation, and Pendulum Operation"; pp. 9-61 in Operational Modes of Agitator Bead Mills, NETZSCH-Feinmahltechnik GmbH, 2003.
7. Web-Site of "Chicago Boiler Company," http://www.cbmills.com, as on 1 June, 2006.

8. D. C. Montgomery, "Design and Analysis of Experiments," pp. 50-86, 3rd Ed. John Wiley & Sons, New York, 1991.
9. G. K. Robinson, Practical Strategies for Experimenting, pp. 12-36, John Wiley & Sons, New York, 2000.
10. R. Moreno, "The Role of Slip Additives in Tape-Casting Technology: Part II-Binders and Plasticizers," *J. Am. Ceram. Soc. Bull.*, **71** [11] 1647-57 (1992).
11. K. Blackman, R. M. Slilaty, and J. A. Lewis, "Competitive Adsorption Phenomena in Nonaqueous Tape Casting Suspensions," *J. Am. Ceram. Soc.*, **84** [11] 2501-06 (2001).
12. J. S. Reed, "Introduction to the Principles of Ceramic Processing," pp. 186-88, John Wiley & Sons, New York, 1988.
13. S. P. Yu, M. C. Wang, and M. H. Hon, "The Dependence of Properties of Alumina-Zirconia-Graphite Refractories on Particle Size Distribution by Furnas Model," *Jpn. J. Appl. Phys.*, **38** 6433-37 (1999).
14. D. H. Yoon and B. I. Lee, "$BaTiO_3$ Properties and Powder Characteristics for Ceramic Capacitors," *J. Ceram. Proc. Res.*, **3** [2] 41-7 (2002).
15. S. W. Kwon and D. H. Yoon, "Effects of Heat Treatment and Particle Size on the Tetragonality of Nano-Sized Barium Titanate Powder," *Ceramics International,* In Press, 2006.
16. Y. Sakabe, N. Wada, T. Hiramatsu, and T. Tonogaki, "Dielectric Properties of Fine-Grained $BaTiO_3$ Ceramics Doped with CaO(*in Jpn.*)," *J. Appl. Phys.*, **41** 6922-25 (2002).
17. S. Wada, H. Yasuno, T. Hoshina, S. M. Nam, H. Kakemoto, and T. Tsurumi, "Preparation of nm-Sized Barium Titanate Particles and their Powder Dielectric Properties (*in Jpn.*)," *J. Appl. Phys.*, **42** 6188-95 (2003).
18. Y. Sakabe, "Recent Development in Multilayer Ceramic Capacitors," pp. 3-15, Vol. 97 in Multilayer Electronic Ceramic Devices. Ceramic Transactions. Ed. by J. H. Jean, T. K. Gupta, K. M. Nair, and K. Niwa, American Ceramic Society, OH, 1998.
19. R. L. Ott and M. Longnecker, "Introduction to Statistical Methods and Data Analysis," 5th Ed. pp. 829-49, Duxbury, CA, 2001.